

Electronic Supplementary Information

Enveloping SiO_x in N-Doped Carbon for Durable Lithium Storage via an Eco-Friendly Solvent-Free Approach

Guangwu Hu,^{‡a} Kunzhe Zhong,^{‡a} Ruohan Yu,^a Zhenhui Liu,^a Yuanyuan Zhang,^a Jinsong Wu,^{ab}

Liang Zhou,^{*ac} and Liqiang Mai^{*ac}

^aState Key Laboratory of Advanced Technology for Materials Synthesis and Processing, Wuhan University of Technology, Wuhan 430070, P. R. China

^bNRC (Nanostructure Research Centre), Wuhan University of Technology, Wuhan 430070, P. R. China

^cFoshan Xianhu Laboratory of the Advanced Energy Science and Technology Guangdong Laboratory, Xianhu hydrogen Valley, Foshan 528200, P. R. China

*Corresponding author: Liang Zhou (Email: liangzhou@whut.edu.cn); Liqiang Mai (Email: mlq518@whut.edu.cn)

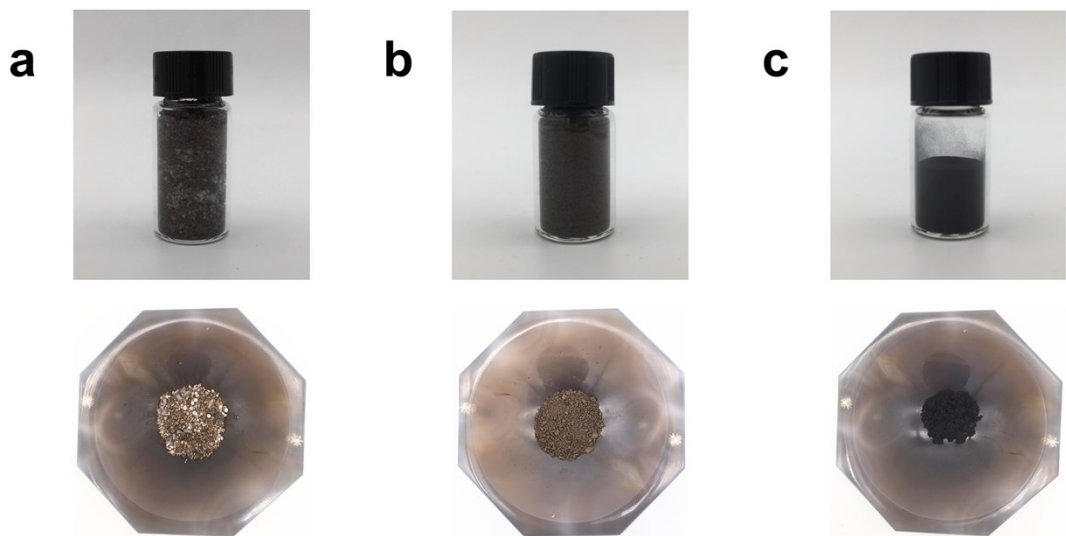


Fig. S1 Digital photos of raw materials before curing (a), $\text{SiO}_x@\text{NC}$ precursor before calcination (b), and $\text{SiO}_x@\text{NC}$ powder (c).

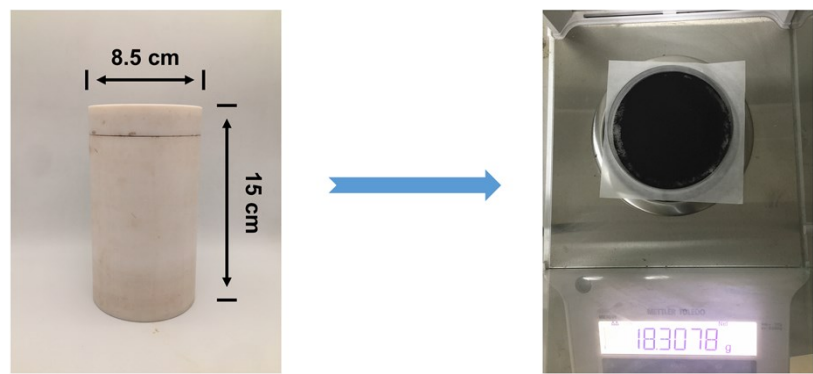


Fig. S2 Digital photos showing the scalable synthesis of $\text{SiO}_x@\text{NC}$.

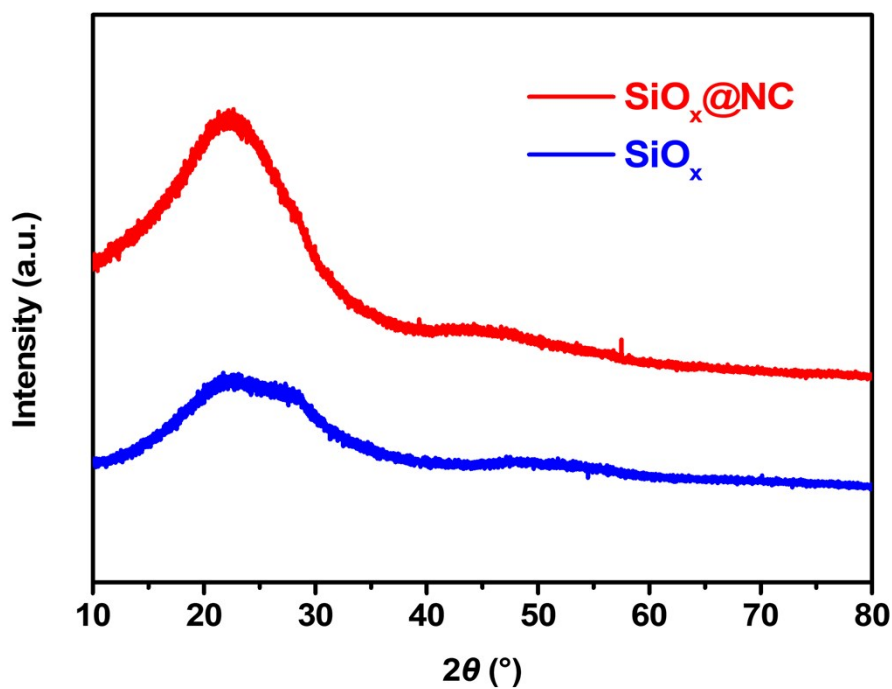


Fig. S3 XRD patterns of $\text{SiO}_x@\text{NC}$ and bulk SiO_x .

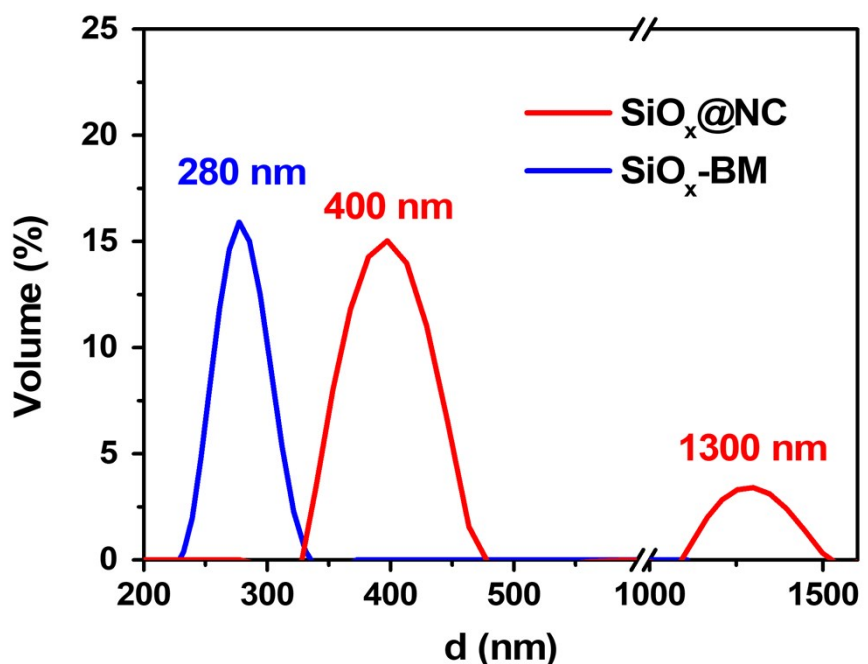


Fig. S4 PSD curves of $\text{SiO}_x\text{@NC}$ and $\text{SiO}_x\text{-BM}$.

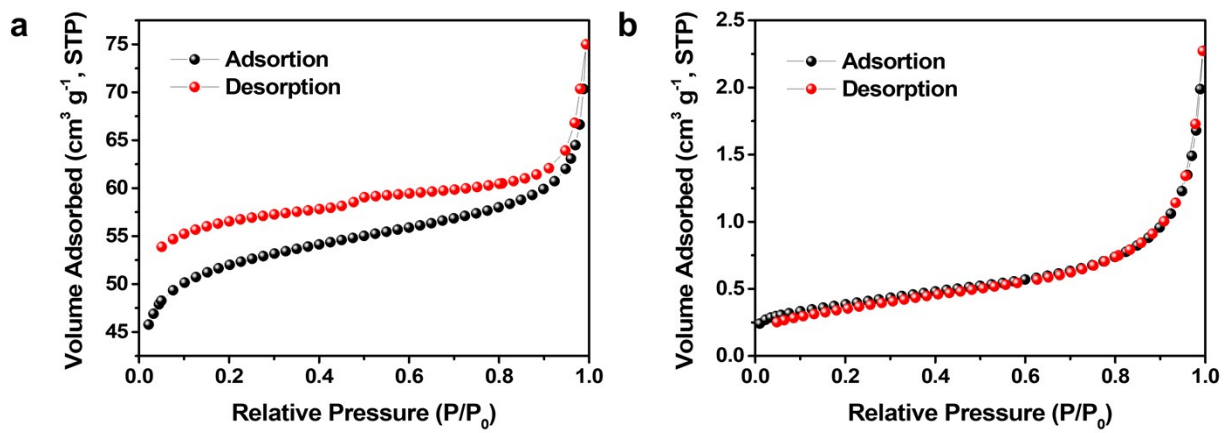


Fig. S5 N₂ adsorption/desorption isotherms of SiO_x@NC (a) and bulk SiO_x (b).

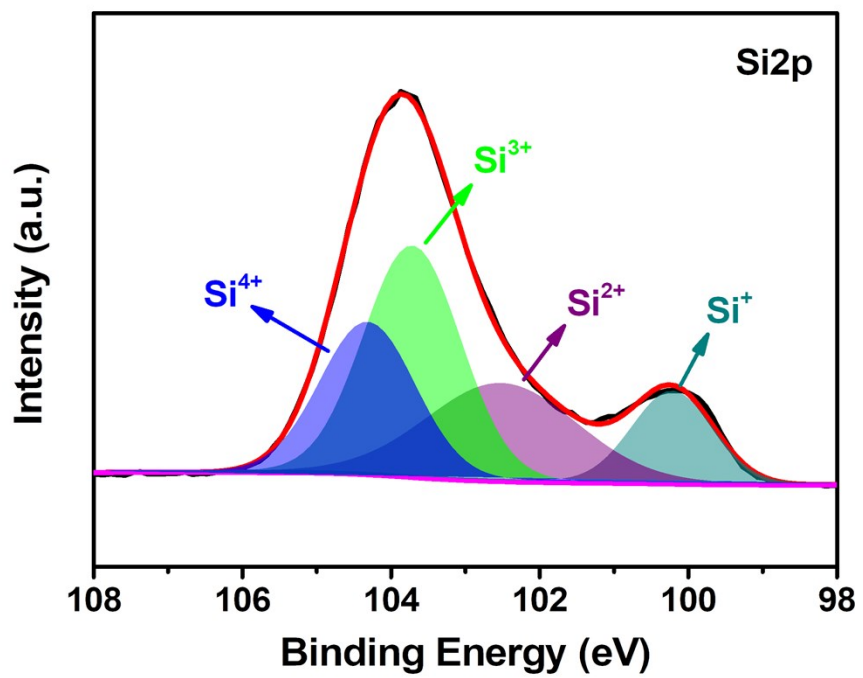


Fig. S6 High-resolution Si2p XPS spectrum of bulk SiO_x .

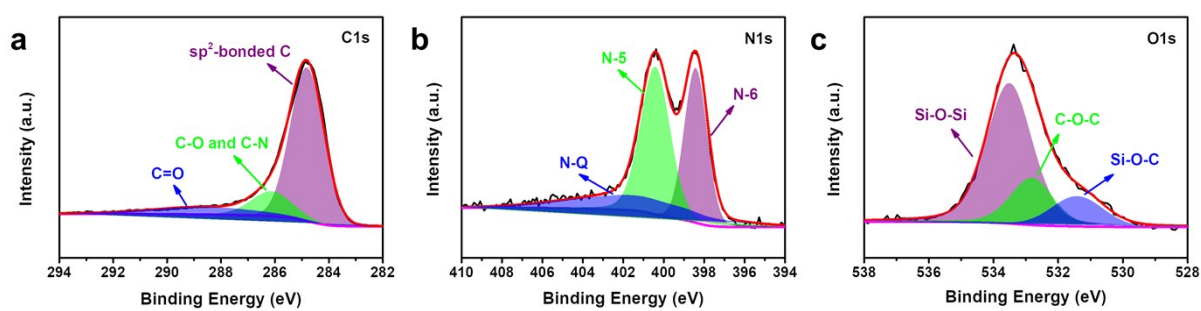


Fig. S7 High-resolution C1s (a), N1s (b), and O1s (c) XPS spectra of $\text{SiO}_x@\text{NC}$.

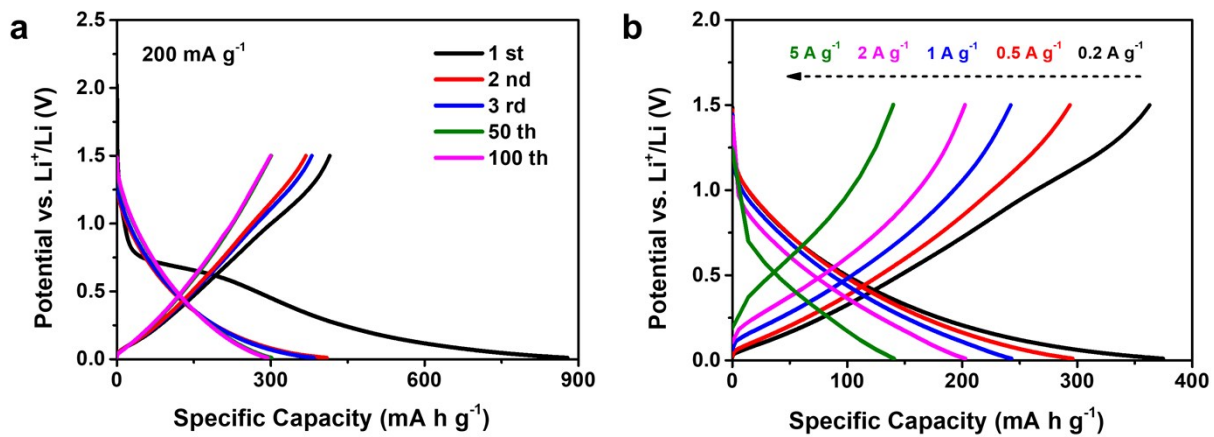


Fig. S8 Selected galvanostatic charge-discharge profiles of NC at 200 mA g^{-1} (a), charge-discharge curves of NC at various current densities (b).

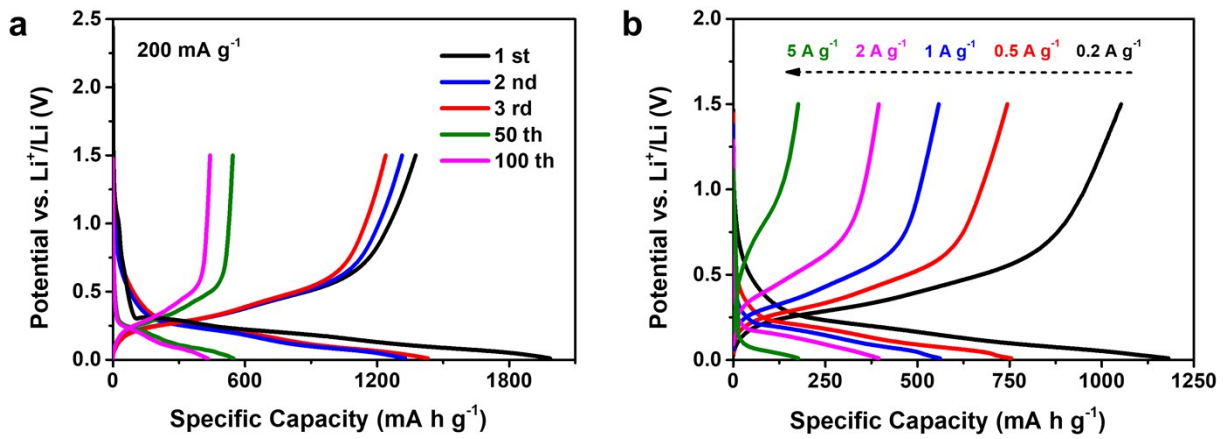


Fig. S9 Selected galvanostatic charge-discharge profiles of bulk SiO_x at 200 mA g^{-1} (a), charge-discharge curves of bulk SiO_x at various current densities (b).

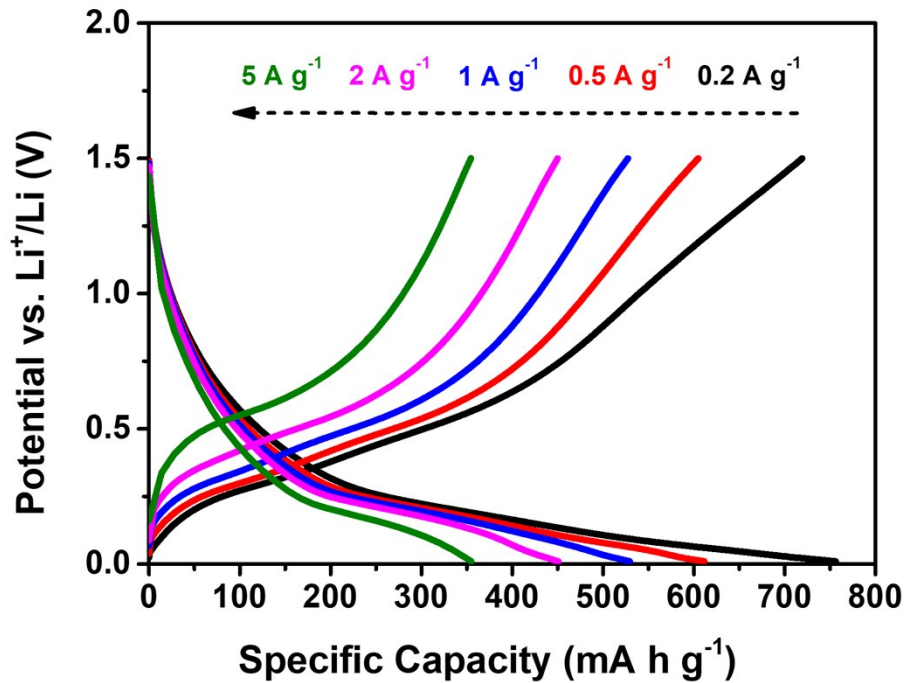


Fig. S10 Charge-discharge curves of $\text{SiO}_x@\text{NC}$ at various current densities.

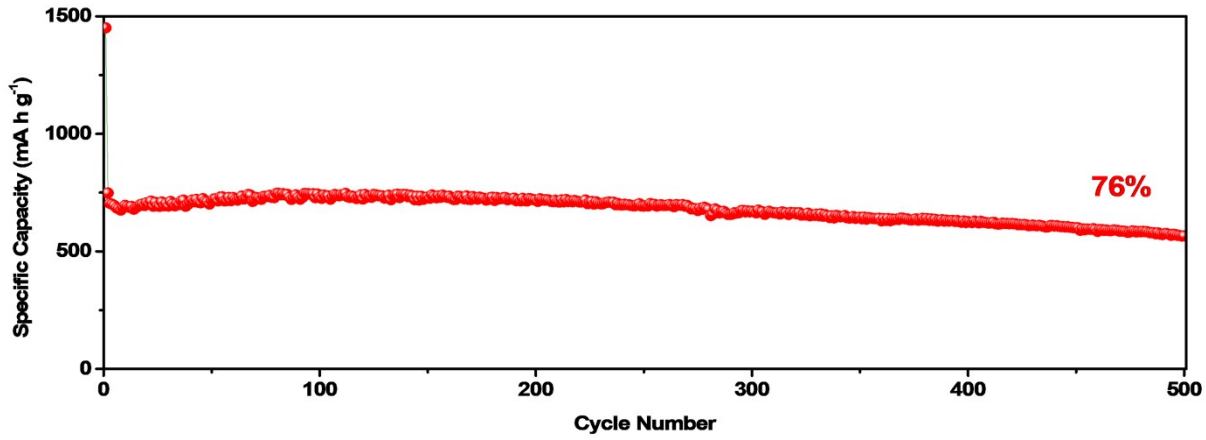


Fig. S11 Long-term cycling performance of $\text{SiO}_x@\text{NC}$ with a lower carbon content at 500 mA g^{-1} .

1.

Tab. S1 Lithium storage performances of various SiO_x -based anode materials.

Ref.	Reversible Capacity (mAh g ⁻¹)	Cycling Performance (mAh g ⁻¹)	Rate Capability (mAh g ⁻¹)	Electrochemical Window
This work	774 (200 mA g ⁻¹)	112 % (500 mA g ⁻¹ , 500 cycles)	345 (5 A g ⁻¹)	0.01 – 1.5 V
[S1]	570 (100 mA g ⁻¹)	\approx 102 % (100 mA g ⁻¹ , 100 cycles)	673 (800 mA g ⁻¹)	0.01 – 2.5 V
[S2]	906 (100 mA g ⁻¹)	\approx 80 % (100 mA g ⁻¹ , 350 cycles)	410 (800 mA g ⁻¹)	0.0 – 3.0 V
[S3]	530 (500 mA g ⁻¹)	\approx 70 % (500 mA g ⁻¹ , 500 cycles)	231 (2 A g ⁻¹)	0.01 – 3.0 V
[S4]	1032 (100 mA g ⁻¹)	\approx 104 % (500 mA g ⁻¹ , 150 cycles)	309 (1 A g ⁻¹)	0.01 – 3.0 V
[S5]	1107 (200 mA g ⁻¹)	\approx 133 % (1 A g ⁻¹ , 1000 cycles)	532 (2 A g ⁻¹)	0.01 – 3.0 V
[S6]	645 (65 mA g ⁻¹)	90 % (325 mA g ⁻¹ , 500 cycles)	549 (3.25 A g ⁻¹)	0.005 – 2.0 V
[S7]	965 (100 mA g ⁻¹)	91 % (500 mA g ⁻¹ , 400 cycles)	620 (600 mA g ⁻¹)	0.01 – 3.0 V
[S8]	1168 (100 mA g ⁻¹)	\approx 99 % (500 mA g ⁻¹ , 500 cycles)	725 (1 A g ⁻¹)	0.01 – 3.0 V
[S9]	653 (120 mA g ⁻¹)	\approx 76 % (300 mA g ⁻¹ , 500 cycles)	582 (3 A g ⁻¹)	0.005 – 2.0 V
[S10]	765 (500 mA g ⁻¹)	79 % (200 mA g ⁻¹ , 200 cycles)	350 (5 A g ⁻¹)	0.01 – 2.0 V

References:

- [S1] P. Lv, H. Zhao, C. Gao, Z. Du, J. Wang and X. Liu, *J. Power Sources*, 2015, **274**, 542-550.
- [S2] Y. Ren and M. Li, *J. Power Sources*, 2016, **306**, 459-466.
- [S3] W. An, J. Fu, J. Su, L. Wang, X. Peng, K. Wu, Q. Chen, Y. Bi, B. Gao and X. Zhang, *J. Power Sources*, 2017, **345**, 227-236.
- [S4] Z. Li, Q. He, L. He, P. Hu, W. Li, H. Yan, X. Peng, C. Huang and L. Mai, *J. Mater. Chem. A*, 2017, **5**, 4183-4189.
- [S5] Q. Yu, P. Ge, Z. Liu, M. Xu, W. Yang, L. Zhou, D. Zhao and L. Mai, *J. Mater. Chem. A*, 2018, **6**, 14903-14909.
- [S6] Q. Xu, J. Sun, Y. Yin and Y. Guo, *Adv. Funct. Mater.*, 2018, **28**, 1705235.

- [S7] Z. Liu, D. Guan, Q. Yu, L. Xu, Z. Zhuang, T. Zhu, D. Zhao, L. Zhou and L. Mai, *Energy Storage Mater.*, 2018, **13**, 112-118.
- [S8] Z. Liu, Y. Zhao, R. He, W. Luo, J. Meng, Q. Yu, D. Zhao, L. Zhou and L. Mai, *Energy Storage Mater.*, 2019, **19**, 299-305.
- [S9] G. Li, J. Li, F. Yue, Q. Xu, T. Zuo, Y. Yin and Y. Guo, *Nano Energy*, 2019, **60**, 485-492.
- [S10] G. Zhu, F. Zhang, X. Li, W. Luo, L. Li, H. Zhang, L. Wang, Y. Wang, W. Jiang, H. K. Liu, S. Dou and J. Yang, *Angew. Chem. Int. Ed.*, 2019, **58**, 6669-6673.

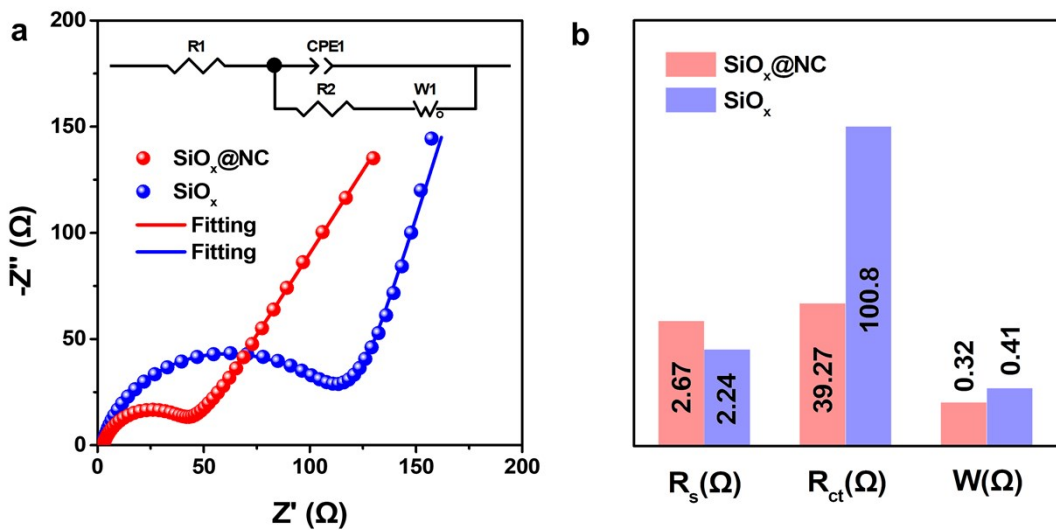


Fig. S12 The electrochemical impedance spectroscopy plots (a) and their results (b) of $\text{SiO}_x@\text{NC}$ and bulk SiO_x before cycling, the inset of (a) is equivalent circuit for fitting impedance plot.

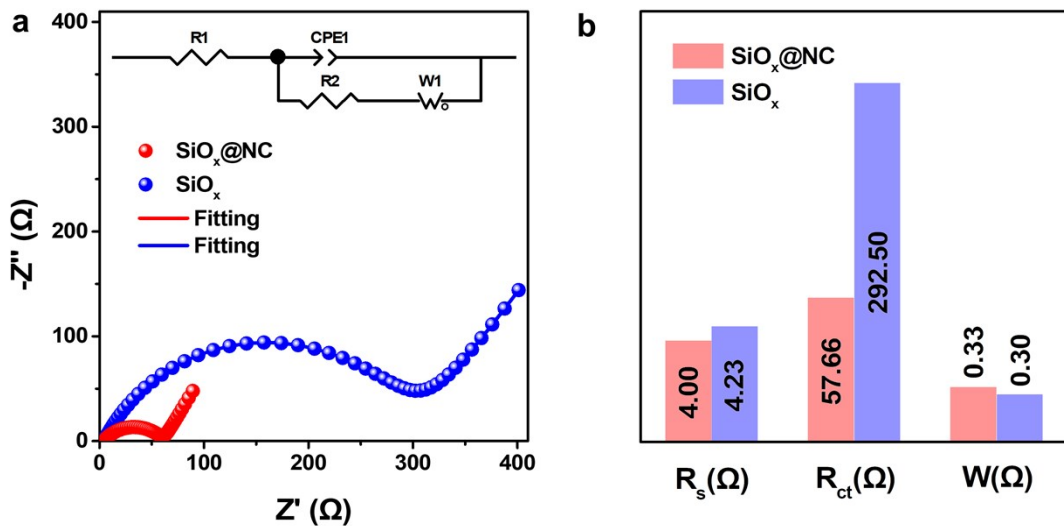


Fig. S13 The electrochemical impedance spectroscopy plots (a) and their results (b) of $\text{SiO}_x@\text{NC}$ and bulk SiO_x after 100 cycles at 200 mA g^{-1} , the inset of (a) is equivalent circuit for fitting impedance plot.

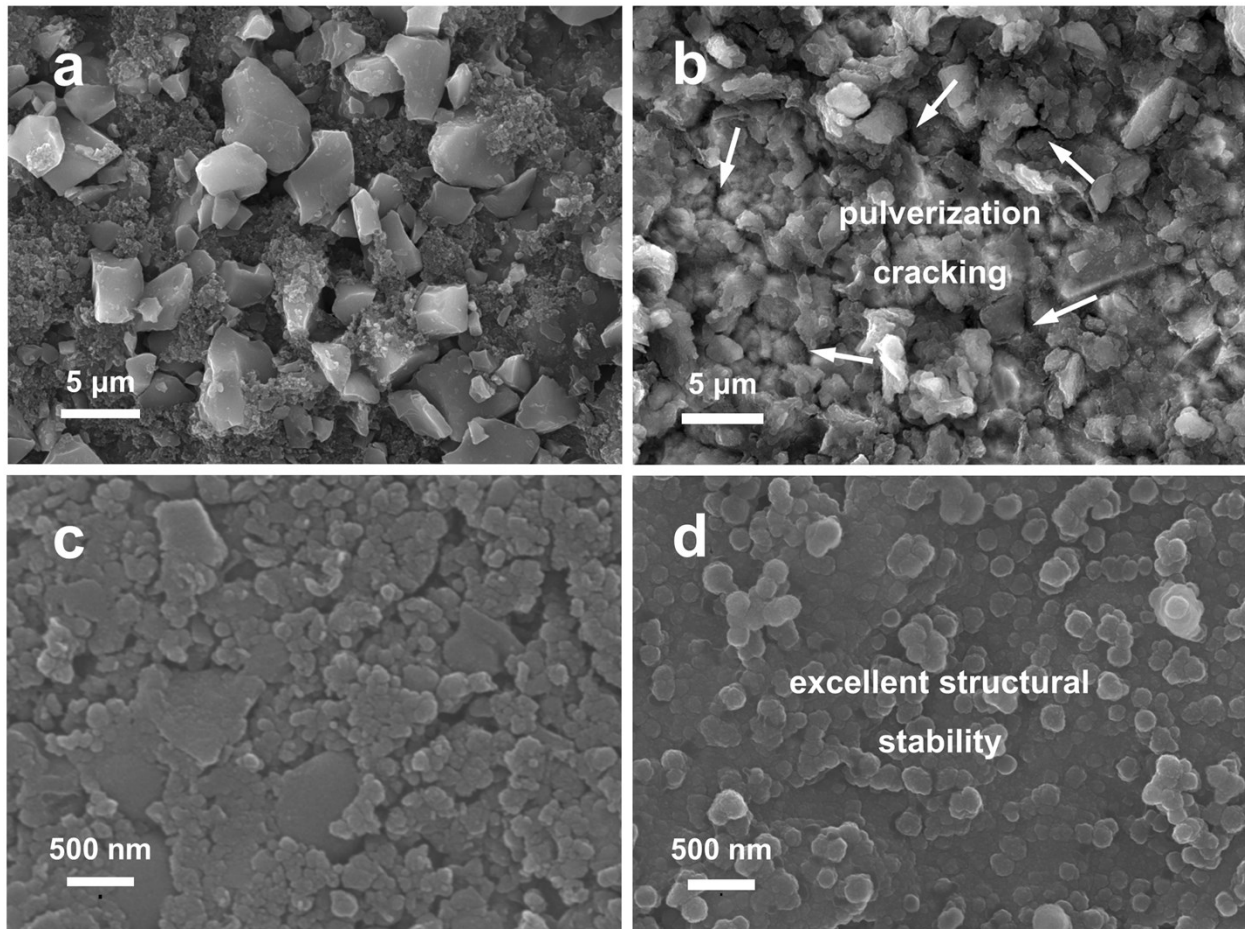


Fig. S14 Top-view SEM images of bulk SiO_x before (a) and after (b) 100 cycles at 200 mA g^{-1} , top-view SEM images of $\text{SiO}_x@\text{NC}$ before (c) and after (d) 100 cycles at 200 mA g^{-1} .

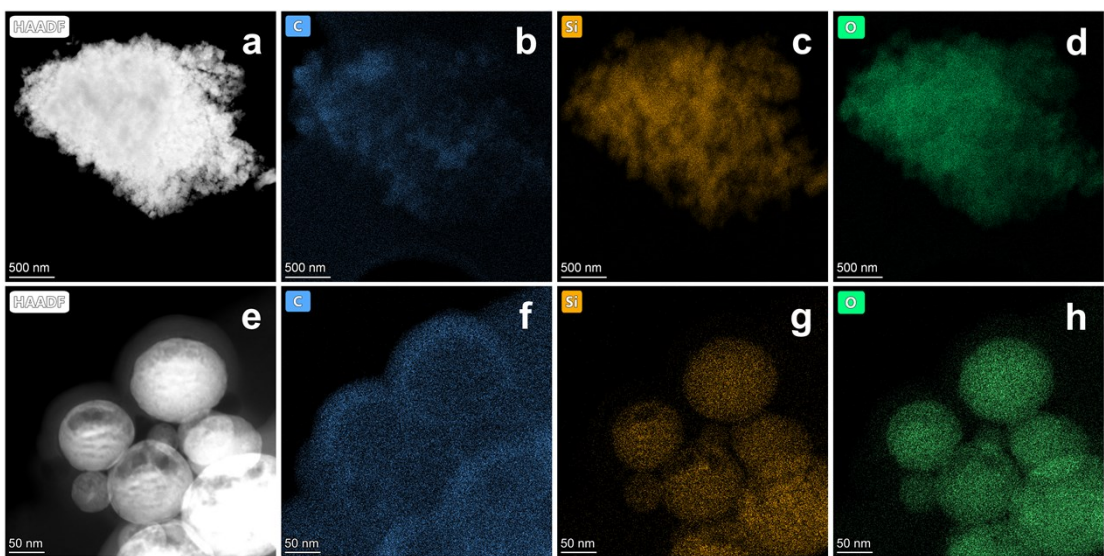


Fig. S15 HAADF-STEM images and EDS mappings of bulk SiO_x (a-d) and $\text{SiO}_x@\text{NC}$ (e-h) after 100 cycles at 200 mA g^{-1} .

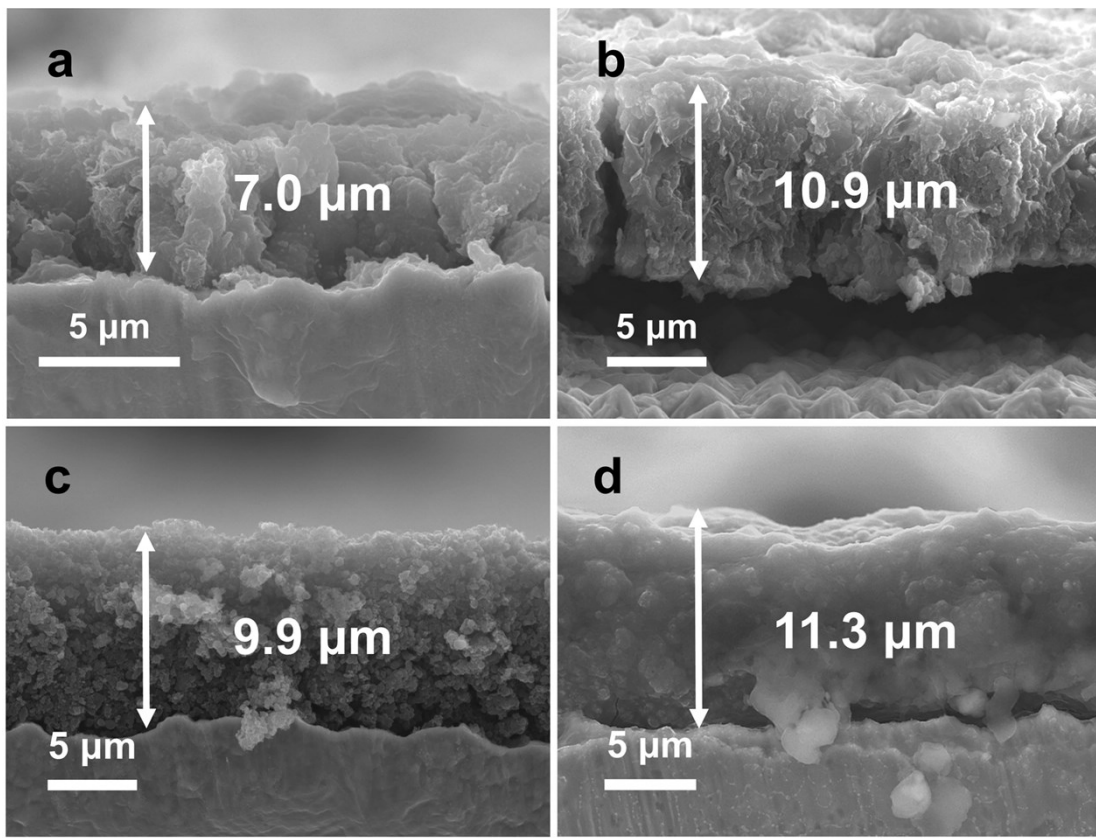


Fig. S16 Cross-sectional SEM images of bulk SiO_x -based electrode before (a) and after (b) 100 cycles at 200 mA g^{-1} , cross-sectional SEM images of $\text{SiO}_x@\text{NC}$ -based electrode before (c) and after (d) 100 cycles at 200 mA g^{-1} .

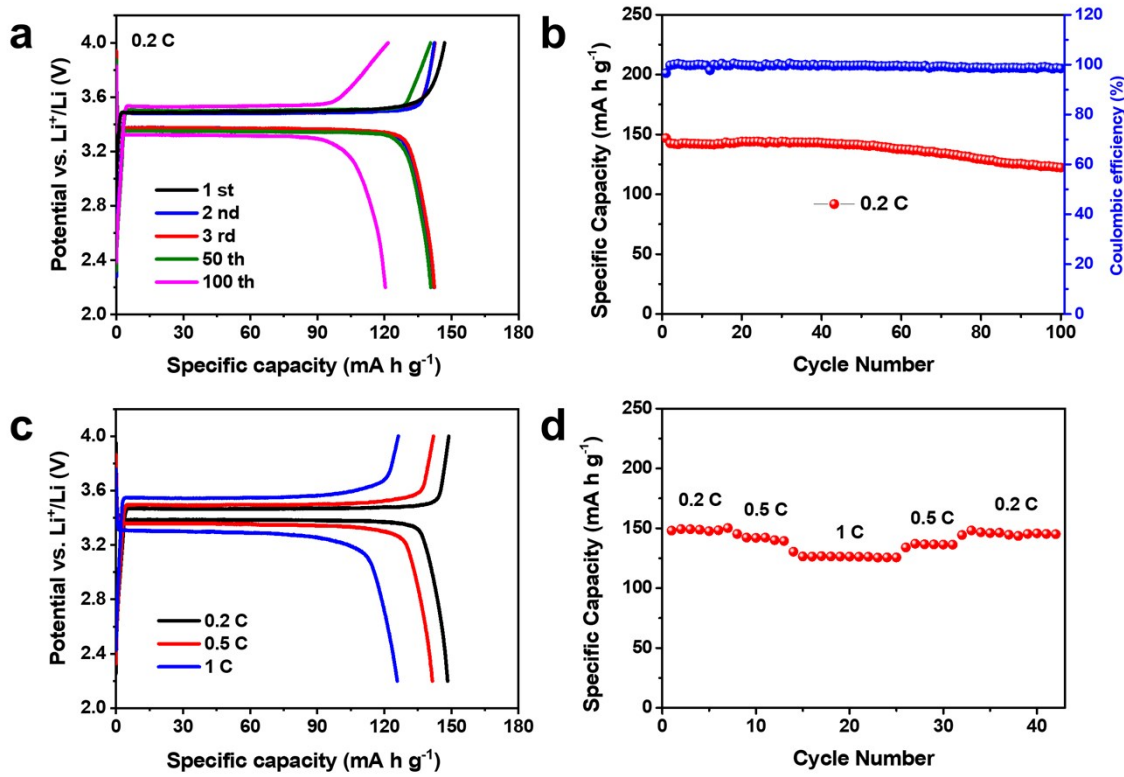


Fig. S17 Selected galvanostatic charge-discharge profiles (a) and cycling performance (b) of LiFePO₄ at 0.2 C (1 C = 170 mA g⁻¹), charge-discharge curves (c) and rate performance (d) of LiFePO₄ at various current densities.